The decarbonisation of petroleum and fossil hydrocarbon fuels for the production and storage of hydrogen

Received 00th January 20xx,
Accepted 00th January 20xx

DOI: 10.1039/x0xx00000x

Xiangyu Jie,[a] Sergio Gonzalez-Cortes,[a] Tiancun Xiao,*[a] Benzhen Yao,[a] Jiale Wang,[b] Daniel R. Slocombe,[c] Yiwen Fang,[a] Noah Miller,[a] Hamid A. Al-Megren,[d] Jonathan R. Dilworth,[a] John M. Thomas,*[e] and Peter P. Edwards*[a]

The importance of petroleum and extracted and refined fossil carbonaceous fuels (petrol, diesel *etc.*) to human society cannot be overestimated. These natural resources have improved billions of lives, worldwide, in providing accessible energy at nearly every scale. Notwithstanding the credible advances in renewable energy production over the past decade or so, the aerial combustion of coal, natural gas and liquid fossil fuels will, given humankinds insatiable demand for power, continue to be the ready source of more than 85% of the world's energy in the foreseeable and possibly the distant future. This combustion of fossil fuels, however, leads to significant anthropogenic emissions of CO_2 to the atmosphere - responsible for over 90% of global CO_2 emissions, - now seen as the major contributor to global warming and climate change. Slowing and ultimately stopping global warming may depend on the ultimate transformation of the global energy system to one that does not introduce aerial CO_2 into the atmosphere. Here we report the production of high volumes of high-purity hydrogen through the catalytic dehydrogenation of petroleum, crude and heavy crude oil and the fossil fuels, petrol, diesel and methane through microwave initiated catalysis of these natural hydrocarbons using microwave-receptive fine and inexpensive iron particles. The co-product of this dehydrogenation process, solid carbon, may be stored in perpetuity or converted to valuable products such as hydrocarbons and other organic materials. Through their catalytic dehydrogenation to yield hydrogen - rather than their aerial combustion- petroleum and fossil fuels can serve as a 'bridge' towards a more distant future when totally carbon-free renewable energy technologies may become more effective and widespread.

Introduction

Petroleum and the extracted and refined hydrocarbon fossil fuels, petrol and diesel are unrivalled in terms of their energy density and ease of use and storage. Such hydrocarbon energy sources can easily be burned in air to produce a copious, easily-controlled evolution of heat[1]. These naturally occurring carbonaceous fuels have increased our comfort, longevity, and affluence. However, it is now recognised that their usage may come at a cost; the aerial combustion of these fuels leads to significant emissions of CO_2 to the atmosphere, estimated at 32.5 giga-tons (Gt) of CO_2 in 2017 alone[2]. Therefore, it is platitudinous to remark that there may be a clear need to shift to alternative fuels, especially from carbon-rich to hydrogen rich fuels[3-5]. One of the principal reasons why progress towards what is recognised as the ultimate of such an energy transition – the hydrogen economy[6-13] - has been so slow, devolves to the fact that there is no readily available massive source of "natural" hydrogen. Furthermore, to date, no reliable means exists for storing hydrogen so that it can be rapidly released – safely, and on demand- for fuel cell and other applications[6, 14-16].

Here, we demonstrate that high purity hydrogen, in high volume, can be rapidly produced using inexpensive iron fine particle catalysts through microwave-initiated, catalytic dehydrogenation of petroleum and other fossil fuels, ranging from extra-heavy crude oil, crude oil through diesel and petrol, and finally to methane.

Results and discussion

At the outset it is important to establish the fundamental differences between conventional and microwave (MW) heating processes, particularly in regard to the heating/ activation of included metal catalyst particles in a host, low thermal conductivity hydrocarbon liquid medium. In a conventional heating process, thermal energy is transferred through convection, conduction and radiation of heat from the outer surfaces of a container into the material itself. In contrast, microwave energy is delivered *directly* to the microwave absorbing/ microwave receptive component through molecular - and in the case of metallic catalyst particles, conduction electron interactions - with the electromagnetic field. In heat transfer by conventional heating, energy is transferred due to developing thermal gradients. However, in microwave heating, electromagnetic energy is transferred, and heat is instead generated, within the sample by electromagnetic coupling through a variety of charge-dynamical processes. We hope to illustrate that this fundamental difference results in important advantages in using microwaves to initiate and promote the catalytic dehydrogenation of

[a.] *King Abdulaziz City for Science and Technology – Oxford Centre of Excellence in Petrochemicals, Inorganic Chemistry Laboratory, Department of Chemistry, University of Oxford, South Parks Road, Oxford OX1 3QR, UK.*
[b.] *Department of Materials, University of Oxford, Parks Road, Oxford, OX1 3PH, UK.*
[c.] *School of Engineering, Cardiff University, Queen's Buildings, The Parade, Cardiff, CF24 3AA, UK.*
[d.] *Petrochemical Research Institute, King Abdulaziz City for Science and Technology, P.O. Box 6086, Riyadh 11442, Kingdom of Saudi Arabia.*
[e.] *Department of Materials Science and Metallurgy, University of Cambridge, 27 Charles Babbage Road, Cambridge, CB3 0FS, UK.*
† Electronic Supplementary Information (ESI) available: [details of any supplementary information available should be included here]. See DOI: 10.1039/x0xx00000x

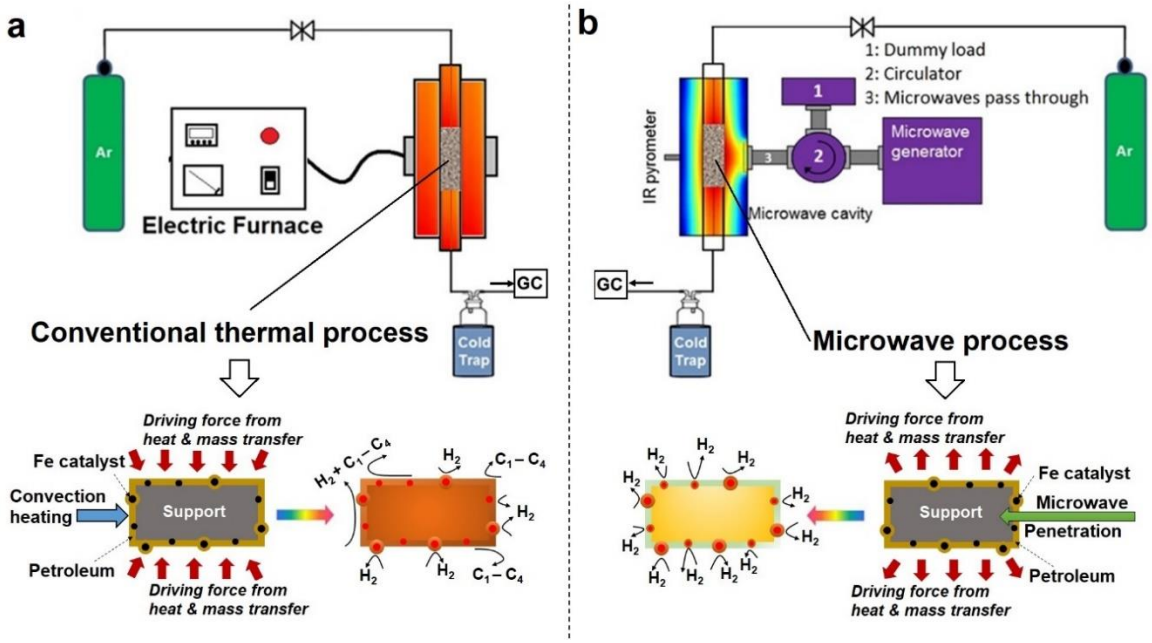

Figure 1. Reaction system configuration (a) a conventional thermal system **(b)** a microwave system. We attempt also to highlight the fundamental differences in the heating processes in both cases and the apparent major differences in catalytic product formation.

hydrocarbon fuels by microwave receptive/ microwave absorbing metal catalyst particles.

The experimental set-up of both conventional thermal process and our purpose-built microwave-catalytic reactor are shown schematically in Figure 1 with further details presented in the Experimental section and also in Supplementary Information; the latter also contains the detailed compositional analysis of petroleum supplied by Saudi Aramco.

Compared to the conventional heating process in which the iron catalyst is gradually heated up by convection heating of the surrounding hydrocarbon fluid, microwave irradiation directly and preferentially interacts with the iron catalysts without significantly heating up the bulk of the hydrocarbon feedstock (Figure 1). This causes a rapid heating of the microwave-absorbing metal catalyst particles themselves and potentially increases the resulting product selectivity. In addition, the applied (fluctuating) microwave field will induce a temperature gradient over the metal catalyst's surface that enhances the molecular diffusion and improves the transport of the active species in a reaction system[17, 18], which subsequently changes the overall reaction rate under microwave conditions as compared with conventional thermal heating.

The difference in the microwave and thermal heating process is also evident in the heat transfer[18]. Under microwave irradiation, the microwave absorbing iron catalyst particle itself heats rapidly and transfers such heat itself to the surrounding support and host fossil fuel medium. In contrast, in a conventional thermal process, the heat transfer to the catalyst particle must be initiated through the surrounding hydrocarbon fluid, being finally transferred to the metal catalyst based purely on convection heating of the "host" low-thermal conductivity hydrocarbon medium. This heat transfer through the hydrocarbon medium finally raises the temperature of an iron catalyst particle to the appropriate catalytic reaction temperature. We will demonstrate that the microwave-initiated catalytic process minimises the catalytic side reactions whilst increasing the selectivity of the hydrogen production (Figure 1). In contrast, under classical convection/ thermal heating, the temperature of the surroundings is higher than the catalyst as the process begins. Thus, the host substance (here the hydrocarbon) could either self-decompose or decompose over the catalyst/ support and this leads to different products in the catalytic process. This important aspect will be demonstrated in our detailed study of diesel dehydrogenation.

Hydrogen production characteristics from petroleum and fossil hydrocarbons

In Figure 2a we show the time-dependent hydrogen evolution arising from the microwave-initiated dehydrogenation of crude and heavy crude oils and various fossil fuels using fine iron catalyst particles (typically 100 nm diameter) on the support materials of either activated carbon (AC) or silicon carbide (SiC). For the simplest comparisons, we used comparable weight % loading levels of the liquid fossil feedstocks on the same support.

Activated carbon is established as an excellent microwave absorber or receptor whilst silicon carbide is characterised by its superior mechanical thermal and dielectric properties which, coupled to exceptional chemical inertness, avoids any complicating issues associated with activated carbon support materials.

Following the initiation of microwave irradiation on the samples, a considerable volume of high-purity hydrogen was readily extracted from the petroleum and heavy liquid feedstocks, typically in periods

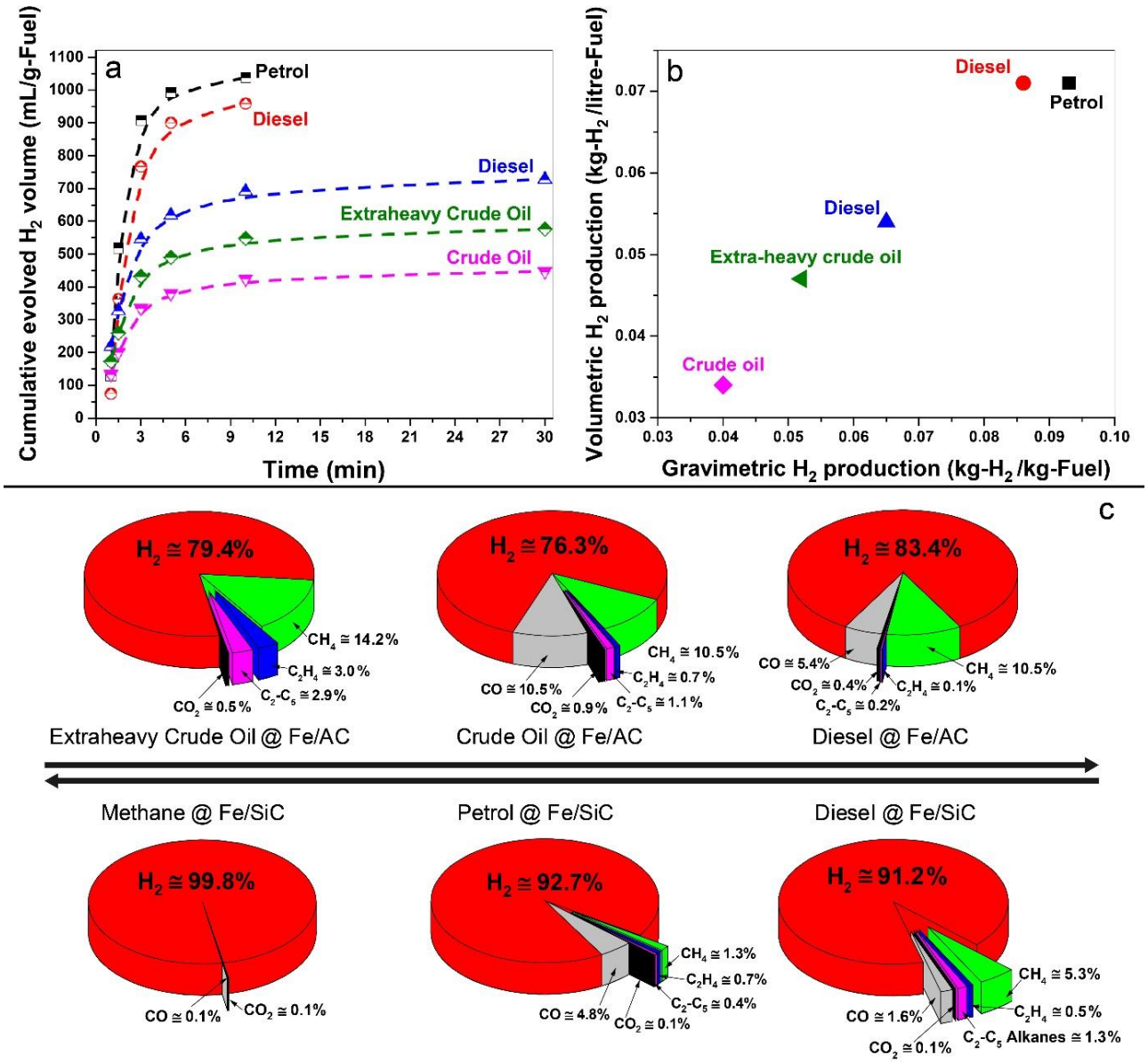

Figure 2. Hydrogen production through the microwave-initiated iron catalysed dehydrogenation of fossil fuels. (a) Cumulative evolved H_2 volume **(b)** H_2 production per volumetric and gravimetric fuel consumption and **(c)** Evolved gas composition of various fossil fuel feedstocks over iron catalysts on silicon carbide (SiC) and activated carbon (AC) under microwave initiation. Samples shown in **(a)** and **(b)** are, black: 30 wt.% petrol @ Fe/SiC, red: 30 wt.% diesel @ Fe/SiC, blue: 40 wt.% diesel @ Fe/AC, magenta: 40 wt.% crude oil @ Fe/AC, olive: 40 wt.% extra heavy crude oil @ Fe/AC.

of about 3 minutes. We find a selectivity of over 90 % for hydrogen in the exiting gas stream following this dehydrogenation of methane, petrol and diesel; selectivity is defined here as the volume % of the product composition of the gaseous products.

For the heavier, and obviously inherently more complex crude and heavy crude oil (see SI), the selectivity of evolved hydrogen is decreased to ca. 75-85 %. Although less hydrogen is produced from these heavy feedstocks, microwave-initiated catalytic dehydrogenation is clearly still highly effective. Due to the inevitable extraneous or residual oxygen contained in the fuel feedstocks (see below), the catalysts and their supports, the production of CO and CO_2 in very low concentrations cannot be avoided under our present experimental conditions[19, 20].

The dehydrogenation of methane to hydrogen and solid elemental carbon reached values of 80% conversion through this microwave-initiated catalytic dehydrogenation process. Corresponding quantitative conversion estimates for petroleum or crude oils are more difficult since they are inherently complex, multicomponent mixtures[21]. For example, petroleum (or crude oil) is a complex, naturally occurring liquid mixture containing mostly hydrocarbons, but also containing some compounds of oxygen, nitrogen and sulphur.

Notwithstanding, we report that hydrogen masses of 0.04, 0.051, and 0.065 kg were extracted from 1 kg of crude oil, extra-heavy crude oil and diesel, respectively, over Fe/AC catalysts (Figure 2b), illustrating the efficacy of the microwave-initiated catalytic

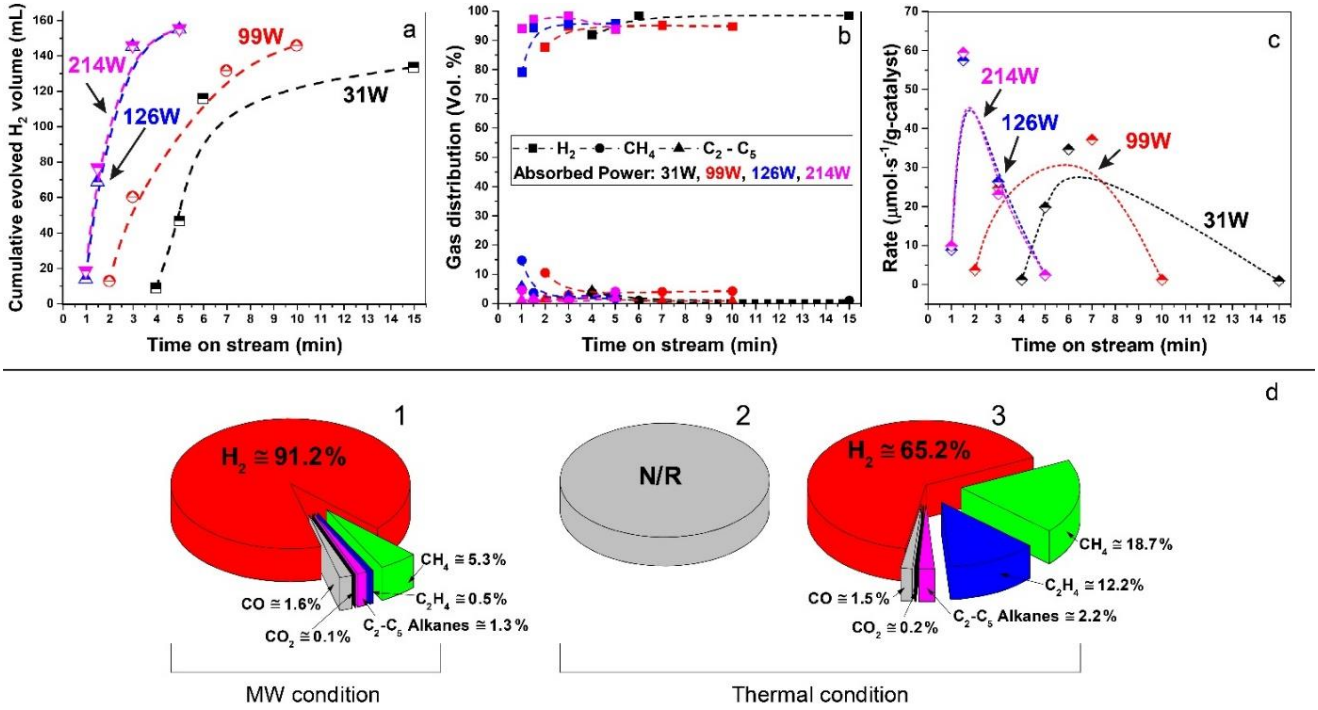

Figure 3. Study of hydrogen production from diesel over 5 wt.% Fe/SiC catalyst under microwave initiation. (a) Cumulative evolved H_2 volume determined by 'time on stream' with different absorbed power. **(b)** The effect of absorbed power on the gas distribution and **(c)** reaction rate of hydrogen production with different absorbed power. **(d)** Comparison of product distribution from diesel @ 5 wt.% Fe/SiC sample under **(d1)** microwave initiation and **(d2, d3)** thermal reactions. **(d2)**, a diesel pre-loaded Fe/SiC sample was subjected to a pre-heated furnace (550 °C), while in the **(d3)**, the Fe/SiC catalyst (without fuel) was pre-heated in the furnace to 550 °C and the diesel was then carefully introduced to the hot catalyst bed by a syringe. The average and the highest temperature recorded under microwave initiation were 416 °C and 568 °C, respectively. 'N/R' indicates no reaction was observed.

dehydrogenation process. Higher levels of hydrogen production, 0.086 and 0.093 kg of hydrogen were liberated from 1 kg of diesel and petrol, respectively, over Fe/SiC catalysts, we will subsequently return to a discussion of these hydrocarbons as hydrogen storage materials themselves.

Parametric studies of the microwave-initiated dehydrogenation of diesel fuel

For detailed studies we chose diesel as a well- characterised fuel product derived from petroleum. The fuel consisted of mainly n-alkanes from C_{12} to C_{21} (89%) with some oxygen containing compounds (11%) such as dodecanol and methyl octadecenoate etc.; all constituents identified by gas chromatography-mass spectrometry (GCMS) (Supplementary Table 1).

Under the microwave-initiated process, diesel fuel was rapidly dehydrogenated over the Fe/SiC catalyst (Figure 2). Hydrogen selectivity exceeded 91% in the evolved gases with less than a fraction of a percent of adventitious CO_2. Small alkanes, mainly methane, comprised ca. 7 vol. % of the remainder of the exit gases.

In Figure 3a, b and c, we show data for 'time-on-stream' experiments for diesel fuel on a Fe/SiC catalyst initiated under various microwave absorbed powers. It can be seen that whilst hydrogen formation rates are strongly dependent upon the incident microwave power levels, hydrogen selectivity itself is not significantly affected by the incident and absorbed microwave power.

Importantly, as with our earlier studies on wax[19], hydrogen evolution ceases *instantly* upon the cessation of microwave irradiation. This is in direct contrast to a conventional thermal heating process, where hydrogen evolution continues to proceed even upon cessation of input heat, as both the catalyst particle and the surrounding "bath" of hydrocarbons slowly cool (Figure 1). Further studies are underway to investigate this important aspect relating to the electromagnetic microwave energy – induced catalyst metal particle- host hydrocarbon ''bath'' interaction. This is a clear illustration that electromagnetic energy from the incident microwaves is being directly – and highly effectively- transmitted to the metal catalyst particles themselves to catalyse hydrogen production.

As shown in Figure 3d, the microwave-initiated catalytic dehydrogenation of diesel produced different levels both of catalytic activity and the (resulting) product selectivities, as compared to the conventional thermal catalytic processes. A stand-out observation, actually common to all the various hydrocarbon feedstocks, is the recurring high selectivity to hydrogen formation under the microwave-initiated catalytic process, as compared to the conventional thermal catalytic dehydrogenation process. We attribute this behaviour once again to the incident microwave electromagnetic energy being selectively, effectively and

preferentially absorbed by the iron catalyst particles as the active catalytic centre, with only modest heating at the outset of the surrounding bulk hydrocarbon fuel by the incoming microwaves. Thus, pure hydrogen is rapidly extracted from the reactant hydrocarbon fuel through the microwave-initiated catalytic reaction at the iron particle surface; this process occurring faster than either the vaporisation of fuel from the heated particle (in our trickle-feed catalyst bed configuration) or the alternative cracking to various hydrocarbons (Figure 1). In contrast, for the corresponding thermal process (Figure 3 d2), rapid vaporisation of the fuel at elevated temperatures predominates before significant catalytic dehydrogenation can occur, with attendant changes also in the resulting product distribution.

In the absence of microwave initiation of the catalytic process, the hydrogen concentration was significantly decreased when we preheated the catalyst bed (using an electrical furnace) before introducing the diesel fuel (Figure 3 d3); under these conditions, higher concentrations of light alkane products were obtained in the evolved gases, suggesting that (conventional) thermal cracking was dominant[22, 23].

In contrast, under microwave initiation, the iron particles themselves are rapidly heated to initiate the catalytic dehydrogenation process. This probably arises since a conventional thermally heated catalytic process produces a multitude of active constituents at the high temperatures of the conventional catalytic process (Figure 1) – these active constituents would include the metal catalyst particles, the support material itself and the hydrocarbon bath itself.

In view of the complex nature of the microwave-initiated heterogeneous catalytic processes involved in this process, at present it is not possible to formulate a complete detailed mechanism for the highly preferential dehydrogenation we observe (Figure 1). Further detailed studies that take into account the nature, and amount, of selective microwave absorption during catalytic turnover are being undertaken. However, what is clear is that this heterogeneous system - hydrocarbon fuel + catalyst - under microwave initiation can lead to non-equilibrium conditions that appear to accelerate endothermic catalytic reactions. In particular, the primary products of the catalytic transformation on the (microwave) heated metal particle surface are quenched rapidly as they leave the metal particle and diffuse into the bulk of the colder reaction mixture surrounding the catalyst, (of course, that hydrocarbon fluid does not itself effectively absorb the microwave energy). It may be the case that products such as hydrogen, atypical product for the conventional (uniform) heating of the catalytic system, can be formed and stabilised. Furthermore, hydrogen corresponds to the stabilised product that very high "local" temperatures – i.e. at the catalyst particle itself - can be rapidly generated under non-equilibrium pyrolytic conditions.

Post-reaction analysis of catalysts

At the completion of our microwave initiation experiments, high-resolution transmission electron microscopy (HRTEM) revealed turbostratic graphitic sheets and multi-walled carbon nanotubes (MWCNTs) that encapsulate both iron and iron carbide nanoparticles. The generation of iron carbide suggested that the supported iron particles react with the hydrocarbon during the catalytic reactions under microwave initiation (Figure 4b, c).

The presence of Fe_3O_4 has also been detected by HRTEM (Figure 4a) in the unreacted catalyst and is considered to form due to the aerial oxidation of nanoparticulate iron. Energy-dispersive X-ray spectroscopy (EDX) mapping also detected the presence of oxygen on some of the iron particle surfaces which could be the source of CO (Supplementary Figure 1).

The formation of iron carbide was also confirmed by X-ray diffraction (XRD) (Figure 5a). The peak of iron at 44.79° was detected in the fresh sample but disappeared after microwave treatment with which the diffraction peaks of Fe_3C was detected in spent samples at

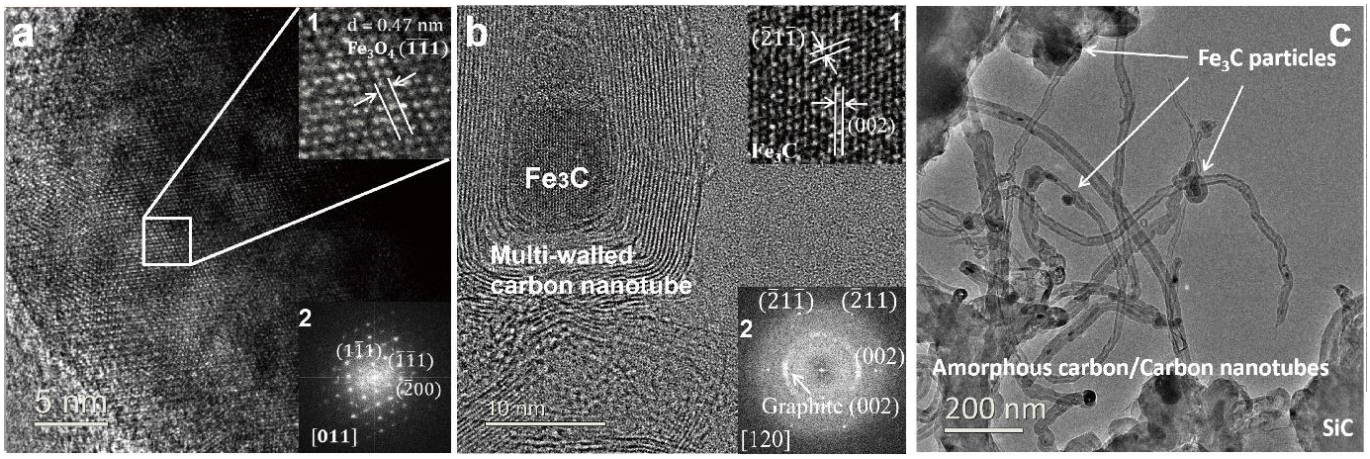

Figure 4. Characterisation of 5 wt.% Fe/SiC catalyst before and after microwave-initiated dehydrogenation of diesel. HRTEM images of **(a)** unreacted catalyst recorded along a <011> zone axis of a Fe_3O_4 particle and **(b)** spent catalyst recorded along a <120> zone axis of a Fe_3C particle. In Figure 4A, the presence of Fe_3O_4 is due to the oxidation of Fe by exposure to air. **(a2)** Diffraction pattern calculated from images of Fe_3O_4 particles of 5 wt. % Fe/SiC, before; and **(b2)** after microwave-initiated catalytic reactions, showing characteristic reflections from graphite (002) plane and Fe_3C along <120> zone axis. **(c)** Low magnification TEM images of produced carbon nanotubes and iron carbide particles in a spent sample.

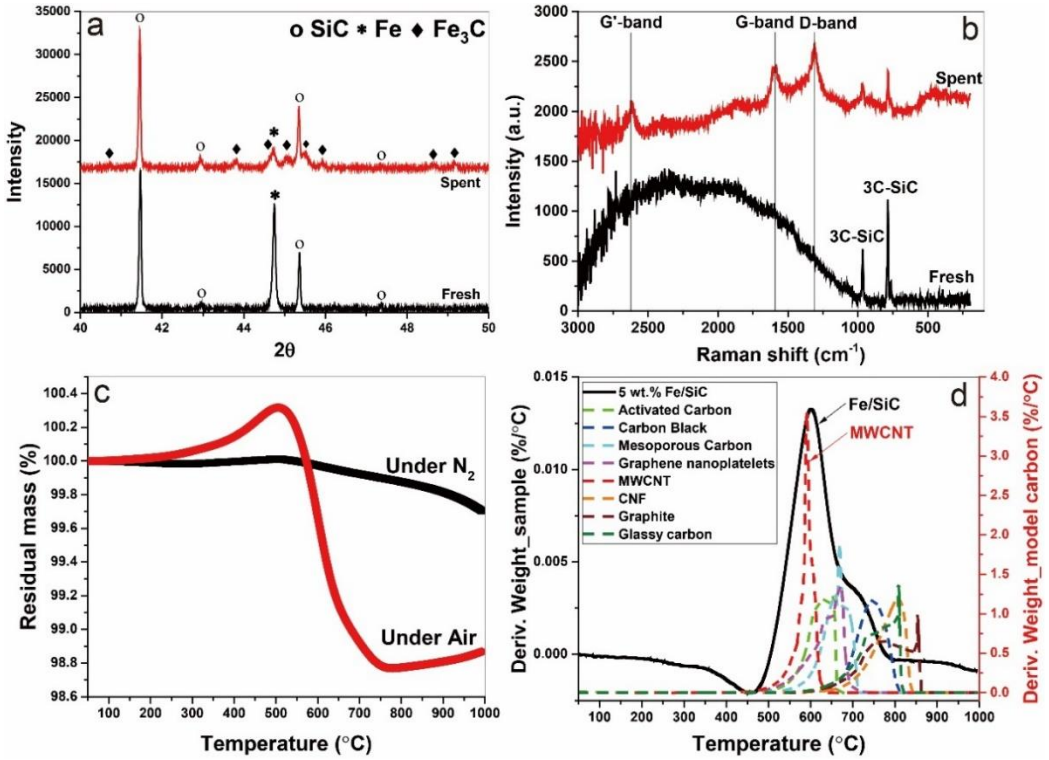

Figure 5. (a) X-ray diffraction (XRD) patterns and **(b)** Raman spectra of 5 wt.% Fe/SiC catalyst. before and after microwave-initiated dehydrogenation of diesel; **(c)** Thermogravimetric analysis (TGA) of spent sample after microwave treatment, the sample was first characterised under nitrogen, and followed by a temperature programmed oxidation; **(d)** Derivative plots of temperature programmed oxidation of spent sample reference to the model carbons.

the angles (2θ) of 42.92°, 43.82°, 44.72°, 45.04°, 45.9°, and 49.18° [24]. Although, no single diffraction peak of carbon was observed in the spent samples, the formation of graphitic carbon and MWCNTs were evident in our HRTEM studies, as well as the Raman spectra, thermogravimetric analysis (TGA) and scanning electron microscope (SEM) (supplementary Figure 2).

Raman spectroscopy reveals characteristic D-band, G-band and G'-band of solid carbon (Figure 5b) in the spent samples. The D-band observed at around wavelength of 1350 cm^{-1} is characteristic of amorphous or disordered carbon, while the peak at about 1580 cm^{-1} (G-band) is ascribed to the vibration of sp^2-bonded carbon atoms in a graphite layer corresponding to ordered graphite carbons. The G'-band peak at around 2700 cm^{-1} is associated with the process of two-photon elastic scattering. The peak intensity ratio of I_G/I_D and $I_{G'}/I_G$ of the spent samples are 0.9 and 0.79, respectively, which suggests the deposited carbon has high carbon nanotubes purity[25]. This is also evident in our thermogravimetric analysis (TGA) when compared to various model carbons.

The TGA study under N_2 atmosphere shows that no intermediates and/or unreacted feedstock were stored in the spent catalysts (Figure 5c). The following temperature programmed oxidation (TPO) illustrated the yield of carbon after single batch test, which is about 2 wt.%. The catalysts can be effectively used for several catalytic cycles through successive additions of fresh feedstock to the reactor system with the growing carbon instantly accumulated on the metal catalyst particle. The oxidation temperature of resulting carbon was referenced to a range of selected model sp^2-bonded carbons (Figure 5d), including activated carbons (ACs), carbon black (CB), graphite, carbon nanofibers (CNFs) and MWCNTs etc. Among these 8 different carbons, the resulting carbon in the spent catalyst has a similar oxidation temperature to MWCNTs at about 593 °C, which also strongly suggests that the majority of carbon produced through this catalytic dehydrogenation is carbon nanotubes. A secondary peak at ca. 700 °C is considered caused by the oxidation of other types of carbon with high content of structural defects.

The utilisation and disposal of carbon by-product residues

Efficient catalytic dehydrogenation of the various hydrocarbon sources and fuels invariably leads to the production of carbon both as a coating ("coking") of the iron catalyst particle (see above) as well as the pure by-product, elemental, solid carbon.

The resulting carbon nanotubes (CNTs) produced from this process potentially has high value and the iron catalysts are basically both inexpensive and abundant. The recycling of the pure co-product carbon for other applications is attractive and a key point that has been outlined by Muradov, Steinberg and co-workers[26-28]. In Figure 6 we identify potential routes for the solid carbon component disposal and utilisation, generated by the process of microwave-initiated fossil fuels dehydrogenation. One possible route is that the carbon can be potentially used as catalysts for other processes (e.g. electrochemistry). Given the fact that the majority of carbon produced during the process are CNTs. Deng *et. al.* previously synthesised a catalyst with iron nanoparticles inside the CNTs[29], that exhibits a high activity and stability towards oxygen reduction reaction (ORR) in polymer electrolyte membrane fuel cells (PEMFC). Moreover, it has been estimated that the direct carbon utilisation by other areas (e.g. building construction materials and soil amendment) could potentially consume very considerable amounts of the carbon by-product[28].

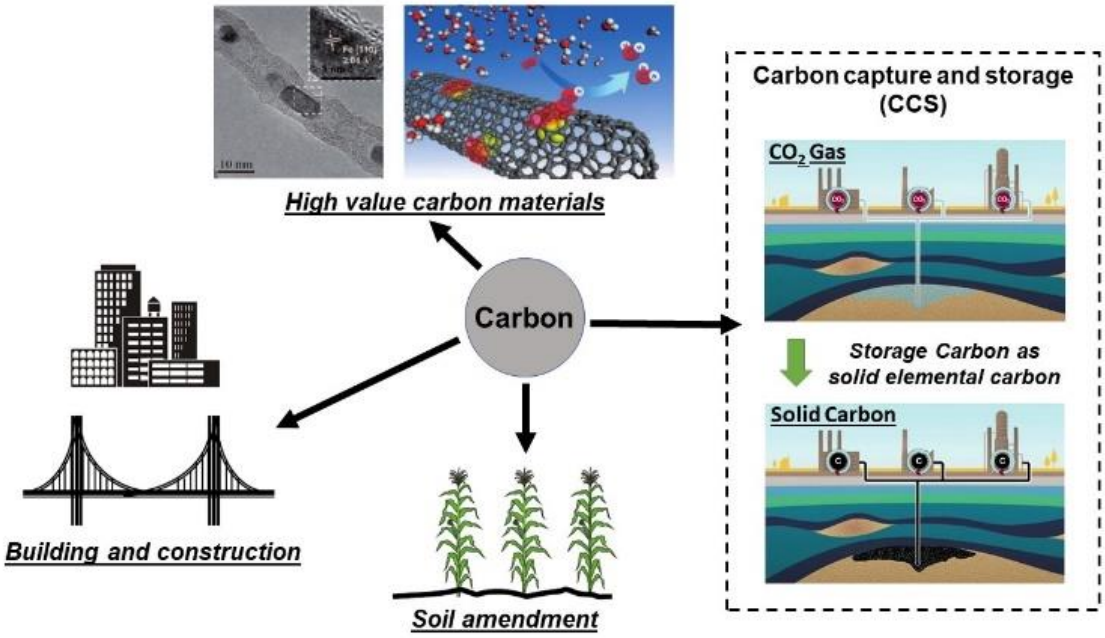

Figure 6. Representative utilisation routes for elemental carbon produced from fossil fuel dehydrogenation, where the hydrogen component of fossil fuels is used as a clean fuel. (Adapted from Ref. 28, 29 and 33).

It is interesting also to draw in and compare the concept of conventional carbon capture and storage (CCS) to prevent the increasing CO_2 level in atmosphere by capturing and storing CO_2 under the ocean or into geologic formations (e.g. depleted oil and gas reservoirs, etc.)[28, 30, 31]. CCS remains an expensive and ecologically uncertain solution; its subsequent capture, transportation and disposal remain costly and the potential hazards associated with underground and oceanic CO_2 sequestration are still uncertain[28, 32, 33]. Thus, an alternative route for CCS, could be achieved by extracting and storing *solid carbon* from our microwave-initiated catalytic dehydrogenation of fossil fuels, leaving the hydrogen to be utilised as clean fuel. As Muradov[28] has noted, it is more attractive - from both a technical and an ecological (and societal) - viewpoint to store elemental carbon underground rather than CO_2. To contrast amounts; take diesel as an example, the complete dehydrogenation of 1 kg diesel to only hydrogen and carbon would generate around 0.961 kg of elemental carbon, whereas the complete aerial combustion of 1 kg diesel will lead to 3.155 kg of CO_2 emission, corresponding to a 1.606 m^3 of CO_2 released to the atmosphere.

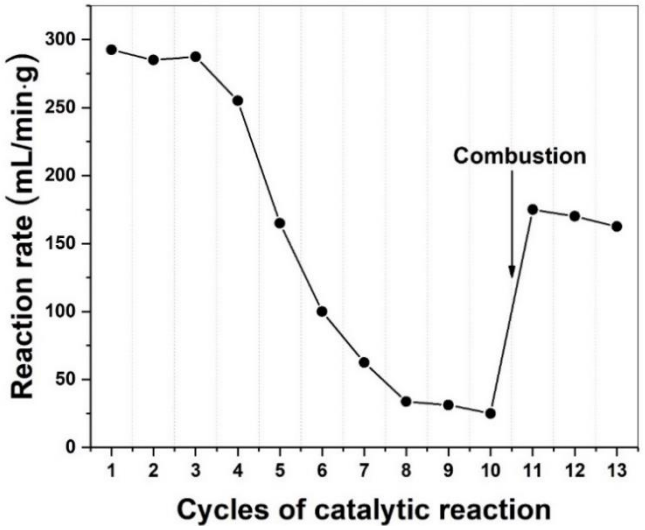

Figure 7. Successive tests on diesel dehydrogenation under microwave irradiation over 5 wt.% Fe/SiC catalysts. 0.5 mL of diesel was refuelled between each cycle and every cycle of tests were run for 10 minutes. The catalyst was recovered by combustion at 550 °C between cycle 10 and 11 in order to remove resulting carbon residues; the catalyst didn't reduce further, and the iron retained as oxides after cycle 11.

The regeneration of metal catalysts

In Figure 7, we present the results of a study to regenerate the iron catalyst activity by removing, through combustion, the build-up of carbon residues following a successive of 10 catalytic cycles. The high initial dehydrogenation rate in catalytic activity gradually diminished and finally transitioned to at a low quasi-steady reaction rate. Following removal of elemental carbon on the catalyst particle by simple combustion after 10 cycles, the catalyst's activity was recovered and remained for several cycles of dehydrogenation. We note that the activity of the catalyst was not fully recovered because of iron oxide presented after the combustion process.

Furthermore, the metal catalysts could also be regenerated through gasification with steam to produce H_2 and CO. Then the syngas can be either separated or used directly as a Fischer-Tropsch feedstock and subsequently recycled back to valuable hydrocarbons. In this process, more H_2 can be produced `and importantly, carbon itself could act as a catalyst under microwave irradiation.

Net Energy Balance considerations

Turning to the important consideration of energy balance, the microwave system is a rather complex system, particularly when combined with absorption of a dispersed heterogeneous catalysis, in a host hydrocarbon medium. Thus, it is difficult to accurately evaluate the efficiency, particularly in a general-use laboratory

microwave cavity device without, for example, impedance matching. Notwithstanding, we attempt to begin to look at the ultimate effectiveness of these hydrogen production processes through evaluation of the "Net Energy Balance (NEB") [19, 34].

The NEB simply means the ratio of energy derived (i.e. the Energy out) from the exiting chemical feedstock (here taken solely as hydrogen and neglecting the chemical energy of co-product solid carbon) to the energy invested (i.e. the Energy in) for the particular process.

Thus, for comparison purposes, we take the NEB here to be the ratio of chemical energy (the *Energy Out*) as the enthalpy of combustion of the hydrogen produced from the fossil fuels, to the energy invested (the *Energy In*) as the electricity power consumption in both the microwave system or the electric furnace.

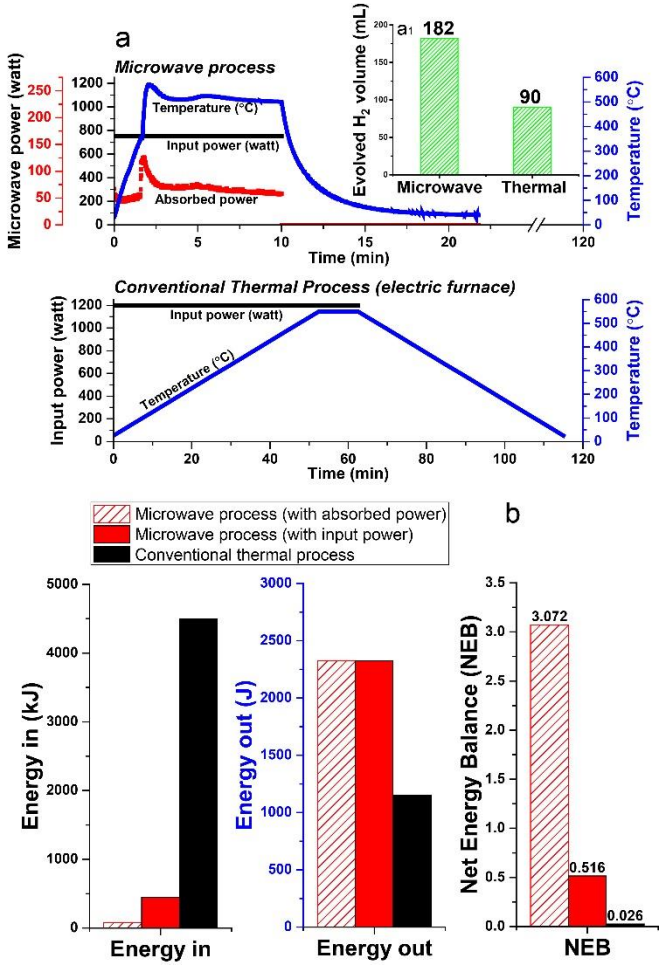

Figure 8. (a) Comparison of microwave process and conventional thermal process for diesel dehydrogenation over 5 wt.% Fe/SiC catalyst. **(b)** Energy balance evaluation between microwave process and conventional thermal process. * The Energy out is calculated as the enthalpy of combustion of the produced hydrogen. Note the differences in time for the two processes with the maximum yield of H_2 in the microwave process occurring after ca. 10min as compared to ca. 60 min for the conventional thermal process **(a1)**.

$$NEB = \frac{Energy\ Out}{Energy\ In} = \frac{Enthalpy\ of\ combustion\ of\ produced\ hydrogen}{Electricity\ consumption} \times 100\%$$

As a preliminary investigation, we also carried out a detailed thermodynamic analysis on the process of the complete dehydrogenation of diesel as a representative hydrocarbon fuel. The theoretical energy required for complete dehydrogenation of diesel to elemental hydrogen and solid carbon is ~1.4 MJ/kg-Diesel and the produced hydrogen has an enthalpy of combustion of ~18.25 MJ/kg-Diesel (Supplementary Table 2). Thus, a very large positive net energy balance can, in principle, be obtained, given a high selectivity in the dehydrogenation process.

However, the NEB ratio is critically dependent on the absorbed microwave power (i.e. the delivered power), thus, the delivery of microwave power to the entire catalytic system and the subsequent conversion need to be further optimised and integrated in order to achieve these theoretical values.

Unfortunately, at present nearly 75 – 90% of the microwave energy used in our small-scale experimental laboratory configuration is lost (Figure 8a and Supplementary Figure 3), quite simply because the high-power microwave device is presently configured only for our very small sample volume (ca. 1.13 cm^3). However, future larger-scale microwave systems would be designed to achieve 99.9% efficient absorbed power and, equally important, renewable sources of primary electricity can be used for the generation of microwaves[35-37]. Such technology optimisation can lead to significant energy savings towards this process.

Notwithstanding these present laboratory limitations, we can show that the microwave –initiated process is energy efficient, as compared to conventional thermal catalytic processes (Figure 8b; full details given in Supplementary Table 3). In this comparison, the corresponding conventional thermal catalytic dehydrogenation process was carried out in an electric furnace. We controlled both processes (microwave + thermal) at a comparable reaction temperature with close to identical amounts of diesel input.

Figure 8a presents the profile of the two processes in terms of the electric input power and temperature. We note again the very short times for hydrogen evolution under microwave-initiation[19], and this represents a highly effective energy transfer process in comparison to the conventional thermal process for heating catalyst particles and the subsequent dehydrogenation process.

In relation to the Net Energy Balance considerations, the Energy Out is taken as the enthalpy of combustion of the produced hydrogen from the two dehydrogenation processes, whereas, the Energy In refers to the electricity power consumption of the two different systems, which are calculated from their tabulated electric power rating and the experiment time of two processes. In the microwave-initiated process, we have also presented the delivered (absorbed) microwave power to give an outlook for a future optimised microwave system (Figure 8b).

It was found that the energy balance of *both* microwave and thermal processes were very low at the laboratory scale set-up,

typically, less than 3%. However, the microwave initiation points to about 20 times higher NEB values as compared to values obtained under conventional thermal process, when one takes into account the time axis of both processes (Figure 8b).

The superior Net Energy Balance of using microwave for hydrogen production is due primarily to the rapid heating and the high activity and selectivity of the fine iron catalyst. Again, it should be noted that in our laboratory configuration, only about 17% of microwave input power was absorbed at the catalyst system used for the dehydrogenation process. The energy balance of the microwave could reach nearly 120 times higher than the thermal process if one considers only the level of absorbed microwave power.

Fossil fuels as hydrogen storage materials

Fossil fuels are themselves excellent hydrogen storage materials since they exceed the targets of H_2 gravimetric and volumetric densities set by the U.S DoE[15, 38]. Our results for the microwave-initiated iron catalysed dehydrogenation of diesel, has shown H_2 gravimetric and volumetric densities of 8.6 kg-H_2/ kg and 71 kg-H_2/ m^3, respectively, exceeding the target of 7.5 kg-H_2/ kg and 70 kg-H_2/ m^3 set by the U.S DoE (Figure 9). Microwave-initiated catalytic dehydrogenation of fossil fuels could become potentially viable for fuel cell vehicles because of three attractive features: First; the rapid production of high-purity hydrogen, highlighted in this study; Second; the necessity for only a small – scale microwave source and reactor system easily attainable for modern high power, small microwave devices for either localized or distributed distribution; and Third; the well-established distribution infrastructure for fossil fuels. Clearly, further studies are needed in both engineering aspects and the optimisation of the entire catalytic process for future applications. Nevertheless, this work clearlly highlights the possible advantages of microwave to assist in the instant generation of high purity hydrogen not only from untreated petroleum products but also from a variety of fossil-derived liquid fuels.

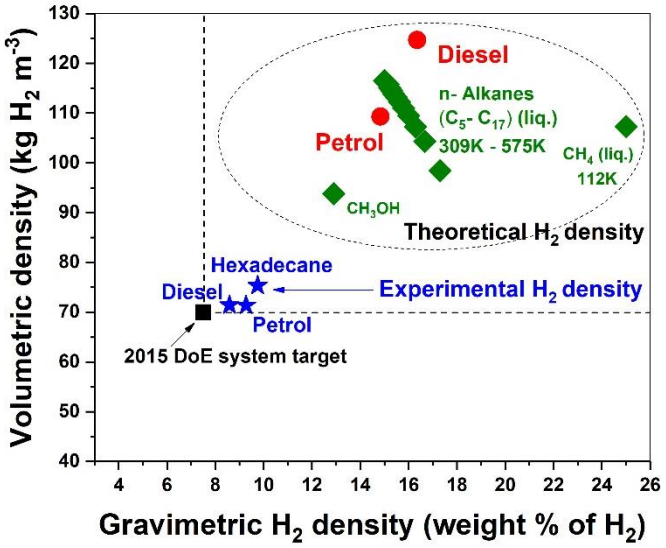

Figure 9. Comparison of theoretical hydrogen density of fossil hydrocarbons with the experimental hydrogen density obtained via microwave-initiated catalytic dehydrogenation of diesel and petrol over 5 wt.% Fe/SiC catalyst.

Concluding Remarks

The work described here illustrates that the microwave-initiated catalytic dehydrogenation of naturally - occurring petroleum, crude oils, and hydrocarbon fossil fuels using inexpensive and abundant fine iron catalysts allows for the rapid production of large volumes of hydrogen.

Fossil fuels produce potentially climate – damaging CO_2 through their aerial combustion. However, we have highlighted the fact that these same fossil fuels could be used to rapidly produce clean hydrogen through their microwave –initiated catalytic dehydrogenation, without the concomitant CO_2 production inevitably associated with their combustion. Based on the advances reported here, it is our belief that the undoubted attractive attributes of fossil fuels - relatively inexpensive, widely available and readily adaptable to applications large and small, simple and complex, - can significantly assist in the staged transition to a hydrogen-based, sustainable hydrogen energy economy. A new scientific and technological era of "*Fossil fuel decarbonisation*'' can arise where we will not destroy naturally-occurring fossil fuels by combustion – fire - conflagration[1] – with the attendant CO_2 emissions, but rather utilise them to produce clean hydrogen. Carbonaceous fossil fuels are thereby transformed from carbon - rich to hydrogen-rich fuels for future energy.

Experimental

Preparation of catalysts

The catalysts used in this study were iron based catalysts and prepared by an incipient wetness impregnation method. Metal nitrates, $Fe(NO_3)_3{\cdot}9H_2O$ (Iron (III) nitrate nonahydrate, Sigma-Aldrich), was used as catalyst precursors whilst SiC (silicon carbide, Fisher Scientific) and AC (activated carbon, Sigma-Aldrich) were used as supports. The supports were mixed with an aqueous solution of iron nitrate, the concentration of which was calculated to produce a desired Fe loading. The mixture was then stirred at 150°C on a magnetic hot plate for 3h until it became a slurry, which was moved into the drying oven and left overnight. The resulting solid mixtures were calcined in a furnace at 350 °C for 3 h. Finally, the active catalysts were obtained by a reduction process in 10% H_2/Ar gases at 800 °C for 6h.

Characterisation of catalysts

The catalysts were carefully characterised before and after experiments by powder X-ray diffraction (XRD, PANalytical X'Pert PRO diffractometer), thermogravimetric analysis (TGA, TA Instrument, SDT Q-600), Laser-Raman spectroscopy (PerkinElmer RamanStationTM 400F spectrometer), scanning electron microscope (SEM, JEOL 840F) and Energy-dispersive X-ray spectroscopy (EDX, ZEISS MERLIN).

The powder X-ray diffraction (XRD) used a Cu Kα X-ray source (45 kV, 40 mA) on a PANalytical X'Pert PRO diffractometer. The scanning range (in 2θ) in this study was 10° to 80°. Thermogravimetric analysis (TGA) was used to characterise the feedstocks remaining and the resulting carbon residue in spent samples. The TGA of spent catalysts was first carried out in an N_2 atmosphere to measure the fuel remaining, the atmosphere was then changed to air to analyse the carbon residue on spent catalysts. The resulting carbon residues were also investigated via Laser-Raman spectroscopy, with laser excitation at 785nm. The scanning electron microscope (SEM, JEOL 840F) was used to characterise the surface morphology of the Fe/SiC catalysts before and after microwave initiation. The surface elemental was analysed by Energy-dispersive X-ray spectroscopy (EDX, ZEISS MERLIN).

The Fe/SiC catalysts were also examined by high-resolution transmission electron microscopy (HRTEM) before and after microwave treatment using JEM-3000F microscope (300 kV). The catalyst powder was dispersed in ethanol in an ultra-sonic bath for 15 min. The solution was then drop cast onto a 300-mesh copper TEM holey carbon grid on a filter paper and allowed to evaporate. Scale bars of all the TEM images were calibrated using an oriented gold crystal grid.

Dehydrogenation process under microwave initiation

The experimental setup is shown in Figure 1b. Microwave system consists of a microwave generation system, a purpose-built microwave cavity and a control system.

The microwave heating system chain prior to the applicator consisted of a power generator, microwave head, microwave circulator, dummy load, microwave power meters and tuneable waveguide sections (Sairem Ltd.). The system was computer controlled using the Labview software. The applicator section was fabricated in the Inorganic Chemistry Laboratory at the University of Oxford. The operating frequency was 2450 MHz ($\pm$ 25 MHz) from 10% to 100% of nominal power. The maximum output power was 2000 W with 1% stability from 10% to 100% of maximum power after thirty minutes on. The microwave source is a magnetron with a ripple rate of < 1% RMS from 10% to 100%. The power rise time is about 100 µs. The power generator is a resonant switching converter with frequencies of 30 kHz up to 80 kHz and an efficiency of 93% at nominal power. The power supply and microwave head are both water and air cooled. The microwave output is via WR 340 waveguides. The generator is controlled remotely via an RS232 MODBUS gateway using the Labview software. The reflected power *R,* was measured by a crystal detector mounted onto the isolator load, from which we determine the power absorbed by the sample, *P*. If the power transmitted to the sample is *W*, then $P = W - R - X$, where *X* is the microwave power being dissipated in the cavity walls and/or being radiated. The applicator used was a TM_{010} resonant cavity to enable a well-characterized field distribution and high nominal field strength. Thus, in this work we investigate electric field driven processes, with a high electric energy density in the sample region[19, 20].

The sample temperature was measured using an infrared (IR) pyrometer, which was also used to control the power to the generator. The pyrometer was positioned horizontally to face a side hole in the microwave cavity. The IR thermometer can only measure the external surface temperature of the catalyst. During the microwave experiment a temperature (T) versus time (t) of reaction profile was recorded. Typically, the power that was delivered to the sample by the microwave radiation and which was dissipated over the sample volume was between 20 W and 200 W[19, 20].

Typically, about 1.13 cm^3 of the catalyst was first placed in a quartz tube (inner diameter 6mm, outer diameter 9 mm) and the height of the catalyst bed exposed to the axially polarised (TM_{010}) uniform electric fields was 4cm. Fuel (about 30 wt.% - 60 wt.% of sample) was then injected into tube and 5-10 minutes was given until the aqueous hydrocarbons were well dispersed into catalysts bed. Then, the filled tube was placed axially in the centre of the TM_{010} microwave cavity to minimise depolarisation effects under microwave radiation. Before starting microwave irradiation, the samples were purged with an Ar flow rate of 1.67 $mL \cdot s^{-1}$ for a period of 15 minutes. Then, the sample was irradiated with microwaves for 30 min at 750 W. The microwave system is not impedance matched, thus the energy delivered to the sample cavity and the microwave power to which the sample was exposed significantly was less than this value. The generated gases were collected and analysed by Gas Chromatography (GC) using a Perkin-Elmer, Clarus 580 GC. The 'escaped' hydrocarbons and the composition of tested fossil fuels were analysed by Gas Chromatograph Mass Spectrometer (GC-MS) using a SHIMADZU, GCMS-QP2010 SE.

Conventional thermal dehydrogenation process

The conventional thermal experiments for diesel dehydrogenation were carried out in an electric furnace for comparison purpose with microwave-initiated experiments. The experimental setup is shown in Figure 1b. The heating rate of electric furnace used in these experiments were 10 °C/min.

The conventional thermal dehydrogenation of diesel was investigated through two different procedures. For one thermal procedure, a diesel pre-loaded Fe/SiC sample was subjected to a pre-heated furnace (550 °C), while in another procedure, the Fe/SiC catalyst (without fuel) was pre-heated in the furnace to 550 °C and the diesel was then carefully introduced to the hot catalyst bed by a syringe.

Conflicts of interest

There are no conflicts of interest to declare.

Acknowledgements

We thank KACST and EPSRC for continued financial support and Dr Afrah Aldawsari and Professor Adrian Porch for their expert assistance in this project. X. Jie gratefully thanks The China Scholarship Council for a scholarship.

Notes and references

1. J. C. Macrae, *An Introduction to the study of fuel*, Elsevier, Amsterdam, 1966.
2. International Energy Agency, *Global Energy & CO_2 Status Report*, 2017.
3. J. M. Thomas, *Nature Catalysis*, 2018, **1**, 2.
4. A. Sartbaeva, V. L. Kuznetsov, S. A. Wells and P. P. Edwards, *Energy & Environmental Science*, 2008, **1**, 79-85.
5. S. J. Davis, N. S. Lewis, M. Shaner, S. Aggarwal, D. Arent, I. L. Azevedo, S. M. Benson, T. Bradley, J. Brouwer and Y.-M. Chiang, *Science*, 2018, **360**, eaas9793.
6. P. P. Edwards, V. L. Kuznetsov, W. I. F. David and N. P. Brandon, *Energy Policy*, 2008, **36**, 4356-4362.
7. S. A. Wells, A. Sartbaeva, V. L. Kuznetsov and P. P. Edwards, *In Encyclopedia of Inorganic and Bioinorganic Chemistry,* R. A. Scott (Ed.)., John Wiley & Sons, New Jersey, 2010. doi:10.1002/9781119951438.eibc0452
8. J. M. Bockris, *Science*, 1972, **176**, 1323-1323.
9. J. A. Turner, *Science*, 2004, **305**, 972-974.
10. U. Eberle, B. Müller and R. Von Helmolt, *Energy & Environmental Science*, 2012, **5**, 8780-8798.
11. K. Hirose, *Philosophical Transactions of the Royal Society of London A: Mathematical, Physical and Engineering Sciences*, 2010, **368**, 3365-3377.
12. L. Barreto, A. Makihira and K. Riahi, *International Journal of Hydrogen Energy*, 2003, **28**, 267-284.
13. J. Barber, *Sustainable Energy & Fuels*, 2018, **2**, 927-935.
14. R. H. Crabtree, *Energy & Environmental Science*, 2008, **1**, 134-138.
15. S. Satyapal, J. Petrovic, C. Read, G. Thomas and G. Ordaz, *Catalysis Today*, 2007, **120**, 246-256.
16. M. L. Wald, *Scientific American*, 2004, **290**, 66-73.
17. C. Antonio and R. T. Deam, *Physical Chemistry Chemical Physics*, 2007, **9**, 2976-2982.
18. S. Horikoshi and N. Serpone, *Microwaves in Catalysis : Methodology and Applications*, Wiley – VCH Verlag GmbH & Co. KGaA, Weinheim, 2016.
19. S. Gonzalez-Cortes, D. Slocombe, T. Xiao, A. Aldawsari, B. Yao, V. Kuznetsov, E. Liberti, A. Kirkland, M. Alkinani and H. Al-Megren, J. M. Thomas and P. P. Edwards, *Scientific Reports*, 2016, **6**, 35315.
20. X. Jie, S. Gonzalez-Cortes, T. Xiao, J. Wang, B. Yao, D. R. Slocombe, H. A. Al-Megren, J. R. Dilworth, J. M. Thomas and P. P. Edwards, *Angewandte Chemie International Edition*, 2017, **56**, 10170-10173.
21. L. R. Radovic and H. H. Schobert, *Energy and fuels in society*, McGraw-Hill Education, New York, 1992.
22. B. Greensfelder, H. Voge and G. Good, *Industrial & Engineering Chemistry*, 1949, **41**, 2573-2584.
23. R. O. Idem, S. P. Katikaneni and N. N. Bakhshi, *Energy & Fuels*, 1996, **10**, 1150-1162.
24. L.-S. Fu, J.-T. Jiang, C.-Y. Xu and L. Zhen, *CrystEngComm*, 2012, **14**, 6827-6832.
25. D. Yao, Y. Zhang, P. T. Williams, H. Yang and H. Chen, *Applied Catalysis B: Environmental*, 2018, **221**, 584-597.
26. M. Steinberg and H. C. Cheng, *International Journal of Hydrogen Energy*, 1989, **14**, 797-820.
27. N. Z. Muradov, *International Journal of Hydrogen Energy*, 1993, **18**, 211-215.
28. N. Z. Muradov and T. N. Veziroğlu, *International Journal of Hydrogen Energy*, 2005, **30**, 225-237.
29. D. Deng, L. Yu, X. Chen, G. Wang, L. Jin, X. Pan, J. Deng, G. Sun and X. Bao, *Angewandte Chemie International Edition*, 2013, **52**, 371-375.
30. M. E. Dry, *Handbook of heterogeneous catalysis*, Wiley – VCH Verlag GmbH & Co. KGaA, Weinheim, 2008.
31. G. P. Van der Laan and A. A. C. M. Beenackers, *Catalysis Reviews – Science and Engineering*, 1999, **41**, 255-318.
32. M. Bui, C. S. Adjiman, A. Bardow, E. J. Anthony, A. Boston, S. Brown, P. S. Fennell, S. Fuss, A. Galindo and L. A. Hackett, *Energy & Environmental Science*, 2018, **11**, 1062-1176.
33. M. E. Boot-Handford, J. C. Abanades, E. J. Anthony, M. J. Blunt, S. Brandani, N. Mac Dowell, J. R. Fernández, M.-C. Ferrari, R. Gross and J. P. Hallett, *Energy & Environmental Science*, 2014, **7**, 130-189.
34. M. Steinberg, *International Journal of Hydrogen Energy*, 1999, **24**, 771-777.
35. Zero Emissions Platform, The Hard Facts behind Carbon Capture and Storage, https://environmentaljusticetv.wordpress.com/2014/10/22/zep-the-hard-facts-behind-carbon-capture-and-storage/).
36. V. G. Gude, P. Patil, E. Martinez-Guerra, S. Deng and N. Nirmalakhandan, *Sustainable Chemical Processes*, 2013, **1**, 1.
37. D. M. Pozar, *Microwave engineering*, John Wiley & Sons, New Jersey, 2009.
38. A. Porch, D. Slocombe, J. Beutler, P. Edwards, A. Aldawsari, T. Xiao, V. Kuznetsov, H. Almegren, S. Aldrees and N. Almaqati, *Applied Petrochemical Research*, 2012, **2**, 37-44.
39. J. Benford, J. A. Swegle and E. Schamiloglu, *High power microwaves*, CRC Press, Florida, 2015.
40. W. Grochala and P. P. Edwards, *Chemcal Review*, 2004, **104**, 1283-1315.

1. J. C. Macrae, *An Introduction to the study of fuel*, Elsevier, 1966.
2. I. E. Agency, *Global Energy & CO2 Status Report*, 2017.
3. J. M. Thomas, *Nature Catalysis*, 2018, **1**, 2.
4. A. Sartbaeva, V. Kuznetsov, S. Wells and P. Edwards, *Energy & Environmental Science*, 2008, **1**, 79-85.
5. S. J. Davis, N. S. Lewis, M. Shaner, S. Aggarwal, D. Arent, I. L. Azevedo, S. M. Benson, T. Bradley, J. Brouwer and Y.-M. Chiang, *Science*, 2018, **360**, eaas9793.
6. P. P. Edwards, V. L. Kuznetsov, W. I. F. David and N. P. Brandon, *Energy Policy*, 2008, **36**, 4356-4362.

7. S. A. Wells, A. Sartbaeva, V. L. Kuznetsov and P. P. Edwards, *Energy Prod. Storage*, 2010, 309-332.
8. J. M. Bockris, *Science*, 1972, **176**, 1323-1323.
9. J. A. Turner, *Science (Washington, DC, U. S.)*, 2004, **305**, 972-974.
10. U. Eberle, B. Müller and R. Von Helmolt, *Energy & Environmental Science*, 2012, **5**, 8780-8798.
11. K. Hirose, *Philosophical Transactions of the Royal Society of London A: Mathematical, Physical and Engineering Sciences*, 2010, **368**, 3365-3377.
12. L. Barreto, A. Makihira and K. Riahi, *International Journal of Hydrogen Energy*, 2003, **28**, 267-284.
13. J. Barber, *Sustainable Energy & Fuels*, 2018.
14. R. H. Crabtree, *Energy & Environmental Science*, 2008, **1**, 134-138.
15. S. Satyapal, J. Petrovic, C. Read, G. Thomas and G. Ordaz, *Catal. Today*, 2007, **120**, 246-256.
16. M. L. Wald, *Sci. Am.*, 2004, **290**, 66-73.
17. C. Antonio and R. T. Deam, *Physical Chemistry Chemical Physics*, 2007, **9**, 2976-2982.
18. S. e. Horikoshi and N. e. Serpone, *Microwaves in Catalysis : Methodology and Applications*.
19. S. Gonzalez-Cortes, D. Slocombe, T. Xiao, A. Aldawsari, B. Yao, V. Kuznetsov, E. Liberti, A. Kirkland, M. Alkinani and H. Al-Megren, *Scientific Reports*, 2016, **6**, 35315.
20. X. Jie, S. Gonzalez-Cortes, T. Xiao, J. Wang, B. Yao, D. R. Slocombe, H. A. Al-Megren, J. R. Dilworth, J. M. Thomas and P. P. Edwards, *Angewandte Chemie International Edition*, 2017, **56**, 10170-10173.
21. L. R. Radovic and H. H. Schobert, *Energy and fuels in society*, McGraw-Hill, 1992.
22. B. Greensfelder, H. Voge and G. Good, *Industrial & Engineering Chemistry*, 1949, **41**, 2573-2584.
23. R. O. Idem, S. P. Katikaneni and N. N. Bakhshi, *Energy & Fuels*, 1996, **10**, 1150-1162.
24. L.-S. Fu, J.-T. Jiang, C.-Y. Xu and L. Zhen, *CrystEngComm*, 2012, **14**, 6827-6832.
25. D. Yao, Y. Zhang, P. T. Williams, H. Yang and H. Chen, *Applied Catalysis B: Environmental*, 2018, **221**, 584-597.
26. M. Steinberg and H. C. Cheng, *International Journal of Hydrogen Energy*, 1989, **14**, 797-820.
27. N. Muradov, *International Journal of Hydrogen Energy*, 1993, **18**, 211-215.
28. N. Z. Muradov and T. N. Veziroğlu, *International Journal of Hydrogen Energy*, 2005, **30**, 225-237.
29. D. Deng, L. Yu, X. Chen, G. Wang, L. Jin, X. Pan, J. Deng, G. Sun and X. Bao, *Angewandte Chemie International Edition*, 2013, **52**, 371-375.
30. M. Bui, C. S. Adjiman, A. Bardow, E. J. Anthony, A. Boston, S. Brown, P. S. Fennell, S. Fuss, A. Galindo and L. A. Hackett, *Energy & Environmental Science*, 2018, **11**, 1062-1176.
31. M. E. Boot-Handford, J. C. Abanades, E. J. Anthony, M. J. Blunt, S. Brandani, N. Mac Dowell, J. R. Fernández, M.-C. Ferrari, R. Gross and J. P. Hallett, *Energy & Environmental Science*, 2014, **7**, 130-189.
32. M. Steinberg, *International Journal of Hydrogen Energy*, 1999, **24**, 771-777.
33. Z. E. Platform, The Hard Facts behind Carbon Capture and Storage, https://environmentaljusticetv.wordpress.com/2014/10/22/zep-the-hard-facts-behind-carbon-capture-and-storage/).
34. V. G. Gude, P. Patil, E. Martinez-Guerra, S. Deng and N. Nirmalakhandan, *Sustainable Chemical Processes*, 2013, **1**, 1.
35. D. M. Pozar, *Microwave engineering*, John Wiley & Sons, 2009.
36. A. Porch, D. Slocombe, J. Beutler, P. Edwards, A. Aldawsari, T. Xiao, V. Kuznetsov, H. Almegren, S. Aldrees and N. Almaqati, *Appl. Petrochem. Res.*, 2012, **2**, 37-44.
37. J. Benford, J. A. Swegle and E. Schamiloglu, *High power microwaves*, CRC Press, 2015.
38. W. Grochala and P. P. Edwards, *Chem. Rev. (Washington, DC, U. S.)*, 2004, **104**, 1283-1315.